ADVANCED MATERIALS
www.advmat.de

The Absence and Importance of Operando Techniques for Metal-Free Catalysts

Yifei Yuan, Matthew Li, Zhengyu Bai, Gaopeng Jiang, Bin Liu, Tianpin Wu, Zhongwei Chen, Khalil Amine, and Jun Lu**

Operando characterization techniques have played a crucial role in modern technological developments. In contrast to the experimental uncertainties introduced by ex situ techniques, the simultaneous measurement of desired sample characteristics and near-realistic electrochemical testing provides a representative picture of the underlying physics. From Li-ion batteries to metal-based electrocatalysts, the insights offered by real-time characterization data have enabled more efficient research programs. As an emerging class of catalyst, much of the mechanistic understanding of metal-free electrocatalysts continues to be elusive in comparison to their metal-based counterparts. However, there is a clear absence of operando characterization performed on metal-free catalysts. Through the proper execution of operando techniques, it can be expected that metal-free catalysts can achieve exceptional technological progress. Here, the motivation of using operando characterization techniques for metal-free carbon-based catalyst system is considered, followed by a discussion of the possibilities, difficulties and benefits of their applications.

1. Introduction

The impact of fossil fuel-based energy sources on climate change has driven immense research efforts into various renewable energy systems. Among them, technologies such as metal-air batteries, fuel cells, and water splitting can help solve the current energy and environmental challenges. The energy conversion and storage in these technologies are dominated by reactions such as hydrogen evolution reaction (HER), hydrogen oxidation reaction, oxygen reduction reaction (ORR), and oxygen evolution reaction (OER), where electrocatalysts are required to enhance the reaction kinetics and improve the overall energy efficiency. Noble metals such as Pt have been widely utilized to promote such reactions and have long proven their usefulness on the historical Apollo and Gemini space missions,[1,2] and even in some public transportation in the past few years.[3] However, the high cost of these precious metals along with other infrastructural reasons have precluded these renewable energy technologies from widespread commercial applications. While cheaper alternatives such as nonprecious transition metals have been researched, their applications have been ultimately hindered by the lack of structural tunability and high susceptibility to corrosion in the acidic environment during hydrogen evolution and CO_2 reduction reaction.[4,5]

Alternatively, researchers have developed metal-free catalyst (MFC). In addition to having a zero-metal content, MFCs have high structural tunability and relatively higher corrosion resistance due to the stable carbon–carbon bonds. Furthermore, MFCs are free from metal dissolution and catalyst poisoning. More importantly, MFCs demonstrate high selectivity and activity from the many potential dopants. The positive effects of introducing heteroatoms atoms into these carbon materials have played an enormous role in advancing MFC. Various dopant species, such as B,[6] N,[2] P,[7] I,[8] and S[9] have dominated the MFC research literature. Over the past decade, the large family of carbon allotropes and dopants have drawn much attention

Dr. Y. Yuan, M. Li, Dr. K. Amine, Dr. J. Lu
Chemical Sciences and Engineering Division
Argonne National Laboratory
9700 Cass Ave, Lemont, IL 60439, USA
E-mail: junlu@anl.gov
M. Li, Dr. G. Jiang, Prof. Z. Chen
Department of Chemical Engineering
Waterloo Institute of Nanotechnology
University of Waterloo
200 University Ave West, Waterloo, Ontario N2L 3G1, Canada

The ORCID identification number(s) for the author(s) of this article can be found under https://doi.org/10.1002/adma.201805609.

DOI: 10.1002/adma.201805609

Prof. Z. Bai
School of Chemistry and Chemical Engineering
Key Laboratory of Green Chemical Media and Reactions
Ministry of Education
Henan Normal University
Xinxiang 453007, China
E-mail: baizhengyu2000@163.com
Prof. B. Liu
School of Chemical and Biomedical Engineering
Nanyang Technological University
62 Nanyang Drive, Singapore 637459, Singapore
Dr. T. Wu
X-Ray Science Division
Argonne National Laboratory
9700 Cass Ave, Lemont, IL 60439, USA

toward ORR,[2,10] OER,[11] CO_2 reduction reaction (CRR),[4] and HER.[5,12] However, the mechanistic understanding is still severely lacking.

Operando techniques are a class of in situ techniques with a specific focus on obtaining characterization data of spatially interesting locations while under analog or even true operating conditions. While in situ techniques only entails characterization under relevant environmental conditions. Although operando characterization has been widely used to study many energy systems, such as lithium-ion,[13] Li–S,[14] and Li–O_2,[15] batteries its application in catalyst technologies has been mostly limited to the metal components. That is to say, there has been nearly no application of operando characterization techniques for understanding the mechanism of MFC electrochemical catalysts. Herein, we will discuss the needs and challenges for the application of operando studies in MFCs. Specifically, we will first justify the necessity of applying such technique by contrasting ex situ and in situ/operando data of electrocatalysis. We will then highlight the key issues in achieving proper operando characterization of MFC-based electrocatalysis and discuss plausible strategies for operando cell designs for bypassing challenges.

2. Necessity of Operando Characterizations in Understanding Electrocatalysis

The two most prominent advantages of operando characterization techniques lie in its ability to reveal both reaction details in real time and to reduce experimental artefacts. Specifically, ex situ methods only provide information regarding the start and end states of targeted material systems, while the stepwise reaction kinetics, the existence of any short-lived intermediates, and the thermodynamic energy landscapes of the overall system are undetectable. In addition, the disturbance to the ongoing reactions by ex situ experiment as well as the chamber-to-chamber sample transfer inevitably introduces artefacts to the data interpretation. To follow, a few examples will be presented to emphasize the different conclusions obtained between ex situ and in situ/operando data.

ORR and OER kinetics in the cathode of a lithium-air battery remains to be elusive due to a lack of in-depth understanding of the reaction details. Particularly, while researchers have found clear evidence of high discharge capacities for RuO_2 catalysts, it remains speculative as to how the supposedly passivated RuO_2 catalyzed any further ORRs that yielded high capacities.[16] In recent years, with the development of operando liquid transmission electron microscopy (TEM), more realistic testing conditions such as the application of a voltage bias with a liquid electrolyte medium, enabled the real-time observation of ORR reactions under realistic catalytic conditions and the correlation of such observations with the simultaneously measured electrochemical potentials.[17] Work by Chen and co-workers implemented scanning transmission electron microscopy (STEM) with a liquid electrochemical cell to investigate the role of RuO_2 as ORR/OER electrocatalyst in Li-O_2 battery.[18] As shown by the "Operando" panel in **Figure 1** (top left),[18,19] it was found that RuO_2 functions as preferential sites for Li_2O_2 precipitation during discharge. More importantly, operando observation clarified that disproportionate reaction plays a major role in the discharge mechanism, which is evidenced by the real-time recording of the formation and growth of isolated/detached Li_2O_2 in the electrolyte around the RuO_2 nanoparticles. For the charge process, prior to such operando studies, the decomposition mechanism of insulating Li_2O_2 (during charge) remained unclear. The detached and poorly soluble Li_2O_2 should presumably be quite inactive in the electrolyte with only the catalytic function of RuO_2 occurring appreciably at the electrolyte-RuO_2-Li_2O_2 triple-phase interfaces. The continuous temporal resolution intrinsic to the operando study of the OER process (top right panel) has offered strong evidence that there should be some comproportionation reaction facilitating the oxidation reaction. The simultaneously measured voltage profile of the liquid cell-based battery during STEM imaging further correlates the electrochemical properties of the system to the real-time structural evolution of targeted cathode particles. Ex situ characterization (bottom panels), on the other hand, only shows static postdischarge and postcharge structures on the surface of RuO_2 nanoparticles without any further catalytic kinetics at various states of (dis)charge as provided by operando characterization. Therefore, it would be nearly impossible to arrive at the same conclusion using ex situ techniques.

As another example, Cu^+ sites on the surface of nanostructures derived from the reduction of copper oxides have long been suggested to be the active sites for CO_2 reduction, while no direct evidence was provided.[20] Using operando X-ray absorption spectroscopy (XAS), Mistry et al. studied the Cu-based catalysts in their working state and finds that Cu^+ is the active species for reducing CO_2 to ethylene by showing that the presence of Cu^+ lowers the onset potential and enhances ethylene selectivity while Cu_2O can still maintain its stability on the surface during CO_2 reduction (**Figure 2**).[21] In contrast, ex situ studies on the similar Cu-based catalyst system obtained no substantial evidence for Cu^+ after the catalysis reactions.[22] The discrepancy between operando and ex situ results might be due to the fact that the ex situ analyses are generally complicated by the inevitable sample removal from the reactors and exposure to atmosphere, as well as the extra sample processing/preparation for ex situ characterizations.[23]

3. Operando Techniques for Metal-Free Catalysts

Similar to metal-based catalyst, some of the main questions for MFC lie in the identification of the reaction intermediates and true active sites. The underlying mechanisms of how heteroatomic doping improve the catalytic performance are believed to be related to the introduction of defects and changes to the electronic states within the carbon matrix.[24] These changes can increase/decrease conductivity or tune the polarity of the carbon substrate and thus diverse the electronic structures of the substrate.[25,26] Yet, there have been barely any convincing experimental data to confirm these proposed mechanisms, severely limiting our ability to design the structure and composition of advanced catalyst candidates. The main difficulty in implementing operando techniques for metal-free catalyst lies in the low atomic weight of the non-metal atoms. These light atoms (C, N, S, O, etc.) are inevitably more difficult to detect

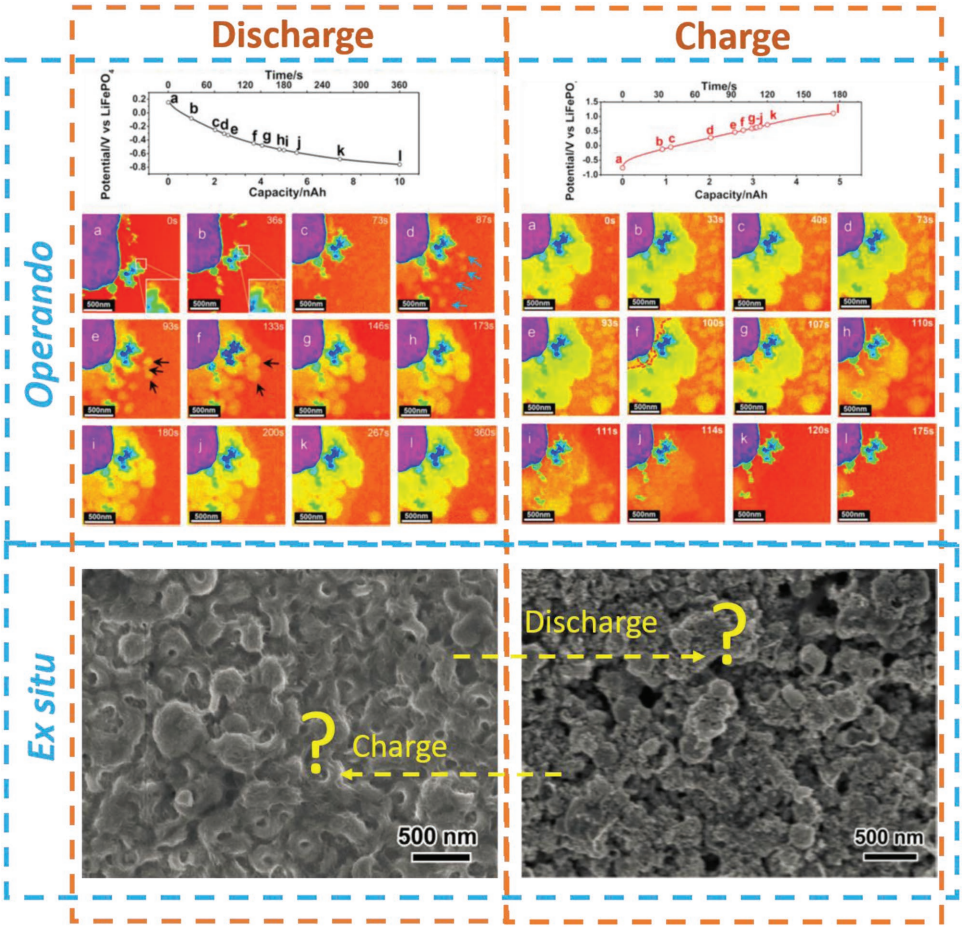

Figure 1. (Top panels) Time sequential high-angle annular dark-field (HAADF)-STEM images showing the formation of Li_2O_2 (in yellow or yellow-green) during ORR and its decomposition during OER catalyzed by RuO_2 nanoparticles (in blue) loaded on Au cathode (in purple). The corresponding voltage profiles measured simultaneously during the operando operation are provided on top. Reproduced with permission.[18] Copyright 2018, Elsevier. (Bottom panels) SEM image of the discharged (left) and charged (right) RuO_2 cathode in the 1st cycle. Reproduced with permission.[19] Copyright 2015, Wiley-VCH. Scale bars in all panels are 500 nm.

due to the small cross section of electron/photon interaction events that are necessary to extract material information.[27] Immediately, hard-XAS can be considered not useful for detecting the elements in MFC, as most dopants are atomically too light. Soft-XAS[28] and X-ray photoelectron spectroscopy (XPS)[29] both have the ability to characterize the doped non-metal atoms' valence. However, both of these techniques are typically operated under high vacuum, making any operando studies difficult. Furthermore, due to the low penetrating power of both XPS and soft-XAS, it is also difficult to collect reliable data through a liquid medium (i.e., electrolyte). Fortunately, recent works in both fields have demonstrated techniques to bypass these experimental hurdles. A soft-XAS study operated under fluorescence mode was achieved by using a ≈100 nm Si_3N_4 barrier to separate a working electrode facing liquid water on one side, from the high vacuum environment of the synchrotron X-ray source on the other. As shown in **Figure 3**a, one side of the working electrode is exposed to liquid electrolyte, while the other side is only separated from a vacuumed XAS measurements environment by a ≈100 nm thin film.[30] XPS techniques have also been reported to operate under a saturated 18–20 Torr of water pressure (equilibrium vapor pressure of water at room temperature),[31] which could potentially enable the operando XPS monitoring of the valency of the MFC atoms. As shown in Figure 3b, the working electrode containing the catalyst is first submerged in an electrolyte solution and then partially raised to allow for a thin 20–30 nm electrolyte film (meniscus) to form. The thin nature of the electrolyte layer allowed for XPS signals to be collected. Such a technique can serve to map out the catalytic process with details pertaining to any sorption process reactants or intermediates to any of the atoms/atomic groups. To the best of our knowledge, these techniques have yet to be applied toward MFC. In these specific examples, the soft XAS system was used to investigate the adsorption of water onto gold, while the XPS system was used to study a Ni–Fe catalyst. However, the general experimental design concepts (separation of vacuum/liquid chambers and decrease rate of liquids evaporation) can serve as very important design criteria for any future MFC operando studies.

For example, the technique of separating the liquid electrolyte from a high-vacuum environment was also leveraged in the aforementioned liquid-cell TEM (Figure 1) and by other groups to achieve more realistic experimental conditions.[15,32] In the case of a liquid TEM cell, two Si chips encapsulating

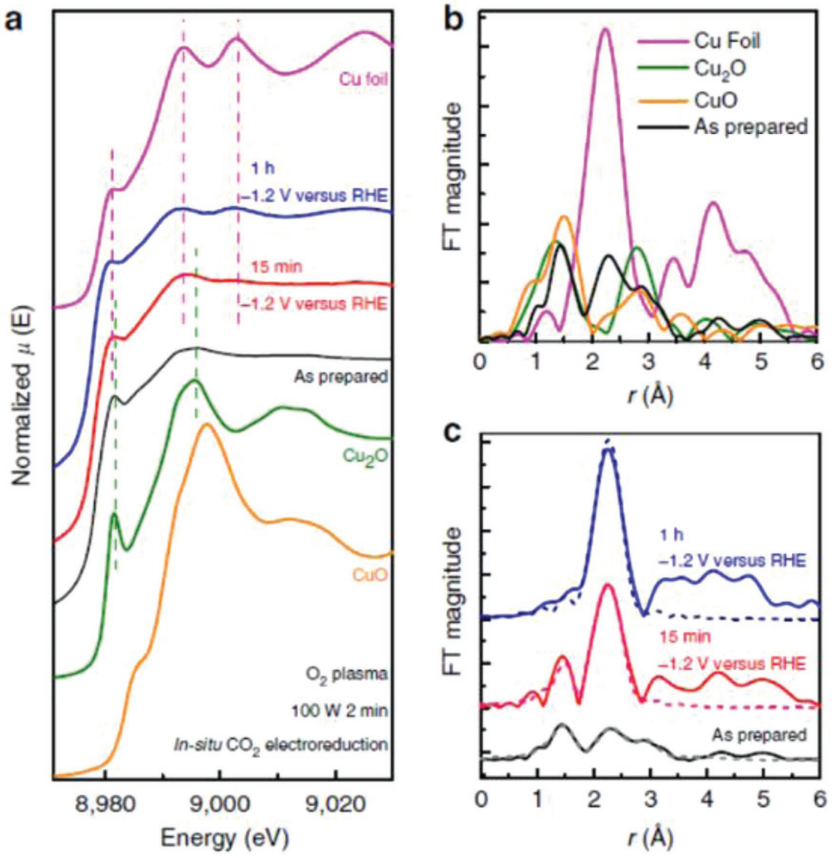

Figure 2. Operando structural and chemical characterization during CO_2 electrochemical reduction. a) X-ray absorption near-edge structure (XANES) spectra of the O_2 100 W 2 min treated sample measured under operando conditions in 0.1 M $KHCO_3$ during the first 15 min and after 1 h of reaction at –1.2 V versus reversible hydrogen electrode (RHE). Bulk Cu, Cu_2O, and CuO spectra are plotted as reference. b) Extended X-ray absorption fine-structure spectroscopy (EXAFS) of the as prepared sample plotted with references. c) EXAFS spectra and fits (dashed lines) of the sample measured under operando conditions. Reproduced with permission.[21] Copyright 2016, Springer Nature.

liquid electrolytes were designed with the imaging area covered by an electron-transparent silicon nitride window of only tens of nanometers in thickness (Figure 3c). However, it might be initially difficult to obtain a TEM image with appreciable contrast as species with low atomic mass might be too convoluted by the compounds in the electrolyte of similar molecular weight. For electron-based techniques, effort should be placed on increasing the cross sections of electron scattering when interacting with light atoms to enhance the signal-to-noise ratio, as well as avoiding sample damage and side reactions caused by incident electrons that possess much higher energy than photons.[33] Our previous work found valuable information pertaining to the interfacial reaction kinetics in an organic electrolyte by optimizing such imaging parameters.[15] While there were no heteroatomic doping on the current collector surface, we still demonstrated the successful nanoscale imaging of light compounds/elements such as Li_2O_2 and even amorphous carbon with improved microscopic contrast. Therefore, from a technical point of view, the reduction in the thickness of the electrolyte layer and the optimization of imaging parameters, such as the accelerating voltage, the size of the imaging area as well as recording time can help to enable the visualization of the atomic dynamics of light elements.[32]

In contrast, neutron scattering can be an excellent technique due to its higher sensitivity to lighter elements. Neutron scattering can distinguish isotopes of lighter elements, enabling the study of proton insertion and elemental absorption among various electrocatalysts.[34] Operando water imaging within the catalyst layer using neutron serves as a noninvasive method to elucidate the catalytic impact of a change in wettability of the carbon support during aging in operating fuel cells[35] Yet, the relatively poor spatial and temporal resolution of this operando approach limits its application range.[36] Furthermore, many techniques are indifferent to the atomic mass of the catalyst. Raman can potentially be used to detect the I_G/I_D ratios of N-doped carbon,[25,37] which can be monitored over cycling to detect any degradation of the nitrogen doping while FTIR can be used to monitor the polar bonds present in C—N, C—O doping and determine chemisorbed processes.[38] Further advancement in these techniques could lead to the use of spectroscopic technique with high spatial resolution. Vibrational spectroscopy (both FTIR and Raman) operated under a high-resolution microscope can provide details on the catalytic process with nanometer resolution.[39] This would provide very powerful information on the state of the catalyst site if an operando configuration can be achieved. However, if this were to be pursued, it would be imagined that a similar XPS cell shown in Figure 3b might be required. Other prospective techniques include the scanning electrochemical microscopy (SECM)[40] and electrochemical quartz crystal microbalance (EQCM). Similar to the Pt-based catalyst, differences in catalytic activity can be differentiated based on different types of atomic doping and defect levels. It has been shown that the defected regions of graphene has a higher activity toward o-phenylenediamine electropolymerization with SECM.[41] EQCM will be able to monitor the mass change of the catalyst electrode as a function of voltage. This technique will provide indirect evidence of the adsorption processes of reactants and intermediates onto the catalyst that occurs prior to the various electrochemical reactions. From this information, a reaction pathway can potentially be drawn, and the catalytic processes can be identified for the various types of MFC.

Finally, beyond general conceptual designs, the specific design of the operando experiment chamber will dictate the usefulness of each characterization technique. For example, if the experimental chamber is required to be sealed for proper operation, a window must be made to allow the detecting beams to reach the samples and be recorded at the detector. In the case of the Si_3N_4 barrier for soft-XAS, the

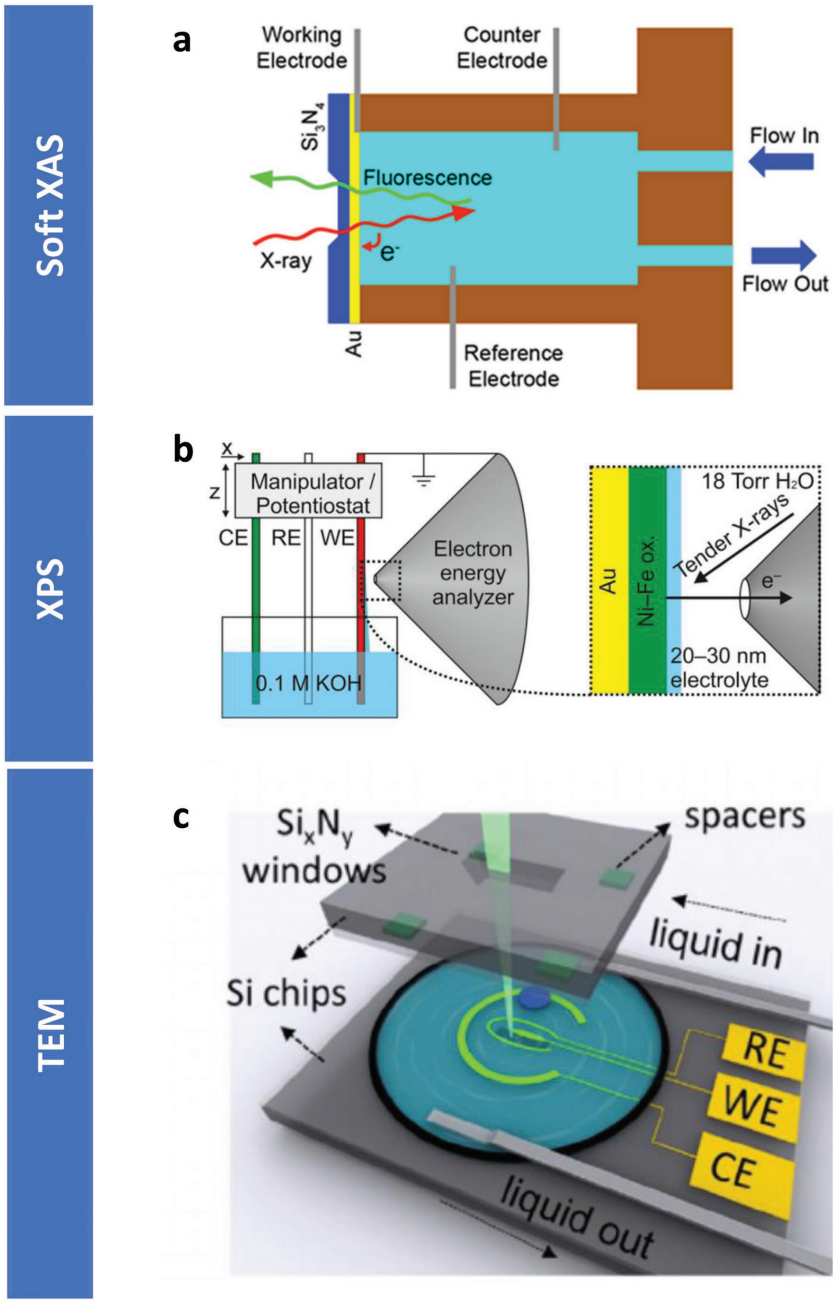

Figure 3. a) Schematic representation of soft XAS (fluorescence mode) cell operated with liquid electrolyte and a ≈100 nm Si_3N_4 film separated the liquid from the vacuum environment. Reproduced with permission.[30] Copyright 2014, the American Association for the Advancement of Science. b) Schematic representation of water saturated XPS experimental setup and c) liquid cell TEM experimental setup with a $LiCoO_2$ counter electrode and carbon working electrode. b) Reproduced with permission.[31] Copyright 2016, American Chemical Society. c) Reproduced with permission.[15] Copyright, 2018 Elsevier.

application of such a thin layer (≈100 nm) was only achieved. Depending on the characterization technique, it is likely that the window must be a part of a sealed cell that can mechanically withstand vacuum conditions and only minutely interact with the signals to be collected by detectors placed outside the chambers.

4. Conclusion

Operando techniques have provided insightful information on the underlying mechanism in metal-based catalyst. It is expected that if the same information is attainable for MFC systems, great advances in MFC technology can be achieved. A more rational selection of catalyst precursors and configuration can thus be made to form new catalysts with desired property and advanced performance. However, the light nonmetal elements are typically difficult to detect, which is further exacerbated by the inevitable accompaniment of electrolytes containing elements of similar atomic weight and even the same atomic species. We have summarized the characterization techniques discussed here in **Table 1**, with details pertaining to their usefulness, foreseeable barriers, and potential solution.

It should be noted that this list is not comprehensive and should only be used as a starting point for future researchers. With the recent trends for application of operando for energy storage research, it is expected that many new techniques will be introduced in the near future. Furthermore, while we can identify a few experimental barriers that can occur for characterizing MFC systems, there will undoubtedly be new experimental challenges that will only become apparent during testing. For example, when operating on the SECM, it is unclear whether the generated gases for both HER and OER will affect the current response or what would be the optimal way (if possible) to inject reduction reactants for ORR and CRR? How would the amount of electrolyte affect the catalyst performance and spectroscopic signal? Furthermore, high-energy probing techniques might change the nature of the material and introduce artefacts.[42] In the future, researchers must take care to identify/eliminate these artefacts to ensure that correct conclusions are drawn. Finally, while speculation can be made about which techniques are the most suitable for MFC and which should be abandoned, ultimately it is the experimentalists' cell design that will determine the final efficacy of these techniques.

Acknowledgements

Y.Y. and M.L. contributed equally to this work. J.L. gratefully acknowledges support from the U.S. Department of Energy (DOE), Office of Energy Efficiency and Renewable Energy, Vehicle Technologies Office. Argonne National Laboratory was operated for DOE Office of Science by UChicago Argonne, LLC, under contract number DE-AC02-06CH11357.

Table 1. List of operando techniques with corresponding function, barriers to application, and possible solutions.

Operando technique	Function	Barriers	Possible solutions
Microscopy			
TEM	Monitor growth of solid phases/change in catalyst morphology	Difficulty in imaging through electrolyte	Optimization of imaging parameters
SECM	Identify most active portions of the catalyst	Unclear	-
AFM	Measure surface potential of catalyst electrode	Low scan rate	Multitip AFM
Mass balance			
EQCM	Monitor adsorbed species on the catalyst electrode	Unclear	-
Spectroscopy			
Raman	Monitor the degree of dopant on the carbon structure over cycling	Signal noise from electrolyte	Unclear
FTIR	Determine the chemisorbed species on catalyst	Transmittance will most likely be impossible	Likely to only work in reflectance mode
XAS	Determine valency of the dopant and carbon.	Lighter elements are hard to detect	Soft XAS, but need to remedy the need for high vacuum
XPS	Determine valency of the dopant and carbon.	Requires high vacuum	Water saturated environment XPS
Scattering			
Neutron scattering	Studying on proton	Low temporal and spatial resolution	Unclear

Z.C., G.J., and M.L. would like to acknowledge financial support from the Natural Sciences and Engineering Research Council of Canada (NSERC) and the Waterloo Institute for Nanotechnology (WIN). Z.B. gratefully acknowledges the financially support from the National Natural Science Foundation of China (Grant No. 21571053), the Program for Innovative Research Team (in Science and Technology) in University of Henan Province (Grant No. 16IRTSTHN004), the 111 Project (Grant No. D17007), Henan Center for Outstanding Overseas Scientists (Grant No. GZS2018003). The authors thank Mr. Boao Song from University of Illinois at Chicago for the help of figure design.

Conflict of Interest

The authors declare no conflict of interest.

Keywords

CO_2 reduction, metal-air battery, metal-free electrocatalysts, operando characterization

Received: August 29, 2018
Revised: September 12, 2018
Published online:

[1] a) M. Winter, R. J. Brodd, *Chem. Rev.* **2004**, *104*, 4245; b) M. Warshay, P. R. Prokopius, *J. Power Sources* **1990**, *29*, 193.
[2] L. Qu, Y. Liu, J.-B. Baek, L. Dai, *ACS Nano* **2010**, *4*, 1321.
[3] a) A. Serov, A. D. Shum, X. Xiao, V. De Andrade, K. Artyushkova, I. V. Zenyuk, P. Atanassov, *Appl. Catal., B* **2018**, *237*, 1139; b) Y. Nonobe, *IEEJ Trans. Electr. Electron. Eng.* **2017**, *12*, 5.
[4] X. Duan, J. Xu, Z. Wei, J. Ma, S. Guo, S. Wang, H. Liu, S. Dou, *Adv. Mater.* **2017**, *29*, 1701784.
[5] Y. Zheng, Y. Jiao, Y. Zhu, L. H. Li, Y. Han, Y. Chen, A. Du, M. Jaroniec, S. Z. Qiao, *Nat. Commun.* **2014**, *5*, 3783.
[6] L. Yang, S. Jiang, Y. Zhao, L. Zhu, S. Chen, X. Wang, Q. Wu, J. Ma, Y. Ma, Z. Hu, *Angew. Chem., Int. Ed.* **2011**, *50*, 7132.
[7] D.-S. Yang, D. Bhattacharjya, S. Inamdar, J. Park, J.-S. Yu, *J. Am. Chem. Soc.* **2012**, *134*, 16127.
[8] Y. Zhan, J. Huang, Z. Lin, X. Yu, D. Zeng, X. Zhang, F. Xie, W. Zhang, J. Chen, H. Meng, *Carbon* **2015**, *95*, 930.
[9] Z. Yang, Z. Yao, G. Li, G. Fang, H. Nie, Z. Liu, X. Zhou, X. a. Chen, S. Huang, *Nano* **2011**, *06*, 205.
[10] a) L. Dai, Y. Xue, L. Qu, H.-J. Choi, J.-B. Baek, *Chem. Rev.* **2015**, *115*, 4823; b) S. Yang, X. Feng, X. Wang, K. Müllen, *Angew. Chem., Int. Ed.* **2011**, *50*, 5339.
[11] a) J. Zhang, Z. Zhao, Z. Xia, L. Dai, *Nat. Nanotechnol.* **2015**, *10*, 444; b) C. Hu, L. Dai, *Adv. Mater.* **2017**, *29*, 1604942.
[12] J. Zhang, L. Qu, G. Shi, J. Liu, J. Chen, L. Dai, *Angew. Chem., Int. Ed.* **2016**, *55*, 2230.
[13] a) C. Zhan, Z. Yao, J. Lu, L. Ma, V. A. Maroni, L. Li, E. Lee, E. E. Alp, T. Wu, J. Wen, Y. Ren, C. Johnson, M. M. Thackeray, M. K. Y. Chan, C. Wolverton, K. Amine, *Nat. Energy* **2017**, *2*, 963; b) J. Lu, T. Wu, K. Amine, *Nat. Energy* **2017**, *2*, 17011.
[14] a) E. C. Miller, R. M. Kasse, K. N. Heath, B. R. Perdue, M. F. Toney, *J. Electrochem. Soc.* **2018**, *165*, A6043; b) G. Li, X. Wang, M. H. Seo, M. Li, L. Ma, Y. Yuan, T. Wu, A. Yu, S. Wang, J. Lu, Z. Chen, *Nat. Commun.* **2018**, *9*, 705.
[15] K. He, X. Bi, Y. Yuan, T. Foroozan, B. Song, K. Amine, J. Lu, R. Shahbazian-Yassar, *Nano Energy* **2018**, *49*, 338.
[16] E. Yilmaz, C. Yogi, K. Yamanaka, T. Ohta, H. R. Byon, *Nano Lett.* **2013**, *13*, 4679.
[17] a) Q. Liu, T. Yang, C. Du, Y. Tang, Y. Sun, P. Jia, T. Shen, Q. Peng, J. Chen, H. Ye, *Nano Lett.* **2018**; b) C. Yang, J. Han, P. Liu, C. Hou, G. Huang, T. Fujita, A. Hirata, M. Chen, *Adv. Mater.* **2017**, *29*, 1702752.
[18] C. Hou, J. Han, P. Liu, C. Yang, G. Huang, T. Fujita, A. Hirata, M. Chen, *Nano Energy* **2018**, 47.
[19] F. Li, D. M. Tang, T. Zhang, K. Liao, P. He, D. Golberg, A. Yamada, H. Zhou, *Adv. Energy Mater.* **2015**, *5*, 1500294.
[20] Y.-J. Zhang, A. A. Peterson, *Phys. Chem. Chem. Phys.* **2015**, *17*, 4505.
[21] H. Mistry, A. S. Varela, C. S. Bonifacio, I. Zegkinoglou, I. Sinev, Y.-W. Choi, K. Kisslinger, E. A. Stach, J. C. Yang, P. Strasser, B. R. Cuenya, *Nat. Commun.* **2016**, *7*, 12123.
[22] C. W. Li, M. W. Kanan, *J. Am. Chem. Soc.* **2012**, *134*, 7231.

[23] X. Li, H. Y. Wang, H. Yang, W. Cai, S. Liu, B. Liu, *Small Methods* **2018**, *2*, 1700395.
[24] X. Zhou, J. Qiao, L. Yang, J. Zhang, *Adv. Energy Mater.* **2014**, 4.
[25] S. Maldonado, S. Morin, K. J. Stevenson, *Carbon* **2006**, *44*, 1429.
[26] L. Panchakarla, K. Subrahmanyam, S. Saha, A. Govindaraj, H. Krishnamurthy, U. Waghmare, C. Rao, *Adv. Mater.* **2009**, *21*, 4726.
[27] S. Findlay, N. Shibata, H. Sawada, E. Okunishi, Y. Kondo, T. Yamamoto, Y. Ikuhara, *Appl. Phys. Lett.* **2009**, *95*, 191913.
[28] a) H. Niwa, K. Horiba, Y. Harada, M. Oshima, T. Ikeda, K. Terakura, J.-i. Ozaki, S. Miyata, *J. Power Sources* **2009**, *187*, 93; b) Y. Gao, G. Hu, J. Zhong, Z. Shi, Y. Zhu, D. S. Su, J. Wang, X. Bao, D. Ma, *Angew. Chem., Int. Ed.* **2013**, *52*, 2109.
[29] a) A. R. MacIntosh, G. Jiang, P. Zamani, Z. Song, A. Riese, K. J. Harris, X. Fu, Z. Chen, X. Sun, G. R. Goward, *J. Phys. Chem. C* **2018**, *122*, 6593; b) X. Fu, F. M. Hassan, P. Zamani, G. Jiang, D. C. Higgins, J.-Y. Choi, X. Wang, P. Xu, Y. Liu, Z. Chen, *Nano Energy* **2017**, *42*, 249; c) K. Gong, F. Du, Z. Xia, M. Durstock, L. Dai, *Science* **2009**, *323*, 760.
[30] J.-J. Velasco-Velez, C. H. Wu, T. A. Pascal, L. F. Wan, J. Guo, D. Prendergast, M. Salmeron, *Science* **2014**, *346*, 831.
[31] H. Ali-Löytty, M. W. Louie, M. R. Singh, L. Li, H. G. Sanchez Casalongue, H. Ogasawara, E. J. Crumlin, Z. Liu, A. T. Bell, A. Nilsson, D. Friebel, *J. Phys. Chem. C* **2016**, *120*, 2247.
[32] Y. Yuan, K. Amine, J. Lu, R. Shahbazian-Yassar, *Nat. Commun.* **2017**, *8*, 15806.
[33] a) T. J. Woehl, K. L. Jungjohann, J. E. Evans, I. Arslan, W. D. Ristenpart, N. D. Browning, *Ultramicroscopy* **2013**, *127*, 53; b) J. M. Grogan, N. M. Schneider, F. M. Ross, H. H. Bau, *Nano Lett.* **2014**, *14*, 359.
[34] a) T. Arlt, W. Lüke, N. Kardjilov, J. Banhart, W. Lehnert, I. Manke, *J. Power Sources* **2015**, *299*, 125; b) P. W. Albers, J. Pietsch, J. Krauter, S. F. Parker, *Phys. Chem. Chem. Phys.* **2003**, *5*, 1941.
[35] R. Satija, D. L. Jacobson, M. Arif, S. Werner, *J. Power Sources* **2004**, *129*, 238.
[36] D. S. Hussey, J. M. LaManna, E. Baltic, D. L. Jacobson, S. Stariha, D. Spernjak, R. Mukundan, R. L. Borup, *ECS Trans.* **2017**, *80*, 385.
[37] J. H. Kaufman, S. Metin, D. D. Saperstein, *Phys. Rev. B* **1989**, *39*, 13053.
[38] A. Misra, P. K. Tyagi, M. K. Singh, D. S. Misra, *Diamond Relat. Mater.* **2006**, *15*, 385.
[39] O. L. Krivanek, T. C. Lovejoy, N. Dellby, T. Aoki, R. Carpenter, P. Rez, E. Soignard, J. Zhu, P. E. Batson, M. J. Lagos, *Nature* **2014**, *514*, 209.
[40] J. L. Fernández, D. A. Walsh, A. J. Bard, *J. Am. Chem. Soc.* **2005**, *127*, 357.
[41] C. Tan, J. Rodríguez-López, J. J. Parks, N. L. Ritzert, D. C. Ralph, H. D. Abruña, *ACS Nano* **2012**, *6*, 3070.
[42] R. Egerton, P. Li, M. Malac, *Micron* **2004**, *35*, 399.